

## Clinical Utility of Body Surface Potential Mapping in CRT Patients

Ksenia Sedova <sup>1</sup>, Kirill Repin <sup>1</sup>, Gleb Donin <sup>1</sup>, Peter Van Dam <sup>2</sup> and Josef Kautzner <sup>3</sup>

1. Department of Biomedical Technology, Faculty of Biomedical Engineering, Czech Technical University in Prague, Kladno, Czech Republic;

2. Department of Cardiology, University Medical Center Utrecht, Utrecht, the Netherlands; 3. Department of Cardiology, Institute for Clinical and Experimental Medicine, Prague, Czech Republic

### Abstract

This paper reviews the current status of the knowledge on body surface potential mapping (BSPM) and ECG imaging (ECGI) methods for patient selection, left ventricular (LV) lead positioning, and optimisation of CRT programming, to indicate the major trends and future perspectives for the application of these methods in CRT patients. A systematic literature review using PubMed, Scopus, and Web of Science was conducted to evaluate the available clinical evidence regarding the usage of BSPM and ECGI methods in CRT patients. The preferred reporting items for systematic reviews and meta-analyses (PRISMA) statement was used as a basis for this review. BSPM and ECGI methods applied in CRT patients were assessed, and quantitative parameters of ventricular depolarisation delivered from BSPM and ECGI were extracted and summarised. BSPM and ECGI methods can be used in CRT in several ways, namely in predicting CRT outcome, in individualised optimisation of CRT device programming, and the guiding of LV electrode placement, however, further prospective or randomised trials are necessary to verify the utility of BSPM for routine clinical practice.

### Keywords

Body surface potential mapping, ECG imaging, heart failure, CRT

**Funding:** This study was supported by the research grant NV18-02-00080 from the grant agency AZV (Ministry of Health of the Czech Republic).

**Disclosure:** JK has received personal fees from Bayer, Biosense Webster, Boehringer Ingelheim, Daiichi Sankyo, Medtronic, Merck Sharp & Dohme, Merit Medical and St Jude Medical (Abbott) for participation in scientific advisory boards; and speaker honoraria from Bayer, Biosense Webster, Biotronik, BMS, Boehringer Ingelheim, Boston Scientific, Daiichi Sankyo, Medtronic, Merck, Merck Sharp & Dohme, Mylan, Novartis, Pfizer, ProMed sro and St Jude Medical (Abbott). PVD is the owner of Peacs BV and ECG Excellence BV. All other authors have no conflicts of interest to declare.

**Received:** 21 March 2021 **Accepted:** 12 May 2021 **Citation:** *Arrhythmia & Electrophysiology Review* 2021;10(2):113–9. **DOI:** <https://doi.org/10.15420/aer.2021.14>

**Correspondence:** Ksenia Sedova, Department of Biomedical Technology, Faculty of Biomedical Engineering, Czech Technical University in Prague, Sitna sq. 3105, 27201 Kladno, Czech Republic. E: [ksenia.sedova@fbmi.cvut.cz](mailto:ksenia.sedova@fbmi.cvut.cz)

**Open Access:** This work is open access under the CC-BY-NC 4.0 License which allows users to copy, redistribute and make derivative works for non-commercial purposes, provided the original work is cited correctly.

Heart failure (HF) is a common condition with significant morbidity and mortality. One of the therapeutic options for advanced management of patients with HF with reduced or preserved left ventricular ejection fraction (HFrEF or HfPEF, respectively) is CRT. In a selected population of candidates, it improves symptoms, quality of life, and prognosis. However, not all patients respond favourably to CRT, which indicates that there are unsolved issues in accurate patient selection and the proper delivery of CRT.<sup>1</sup> Several characteristics predict improvement in morbidity and mortality, and the extent of reverse remodelling is one of the most important mechanisms of action of CRT. Of the clinical parameters, QRS duration is always used as an outcome parameter in all available trials, but consensus has not been reached regarding the optimal ECG-based criteria for patient selection for a CRT device.

The strategy for CRT device optimisation also remains challenging. The available methods include echocardiography, ECG QRS-based assessment, invasive haemodynamic measurements, and/or non-invasive cardiac mapping.<sup>2</sup> Among others, ECG imaging (ECGI) may be a comprehensive tool for measuring ventricular electrical dyssynchrony.<sup>3–5</sup> However, the results are fragmentary and have not been summarised. This paper reviews the current knowledge on non-invasive ECG mapping

methods for patient selection, left ventricular (LV) lead positioning, and optimisation of CRT programming, to determine the major trends and future perspectives for the application of these methods in CRT patients.

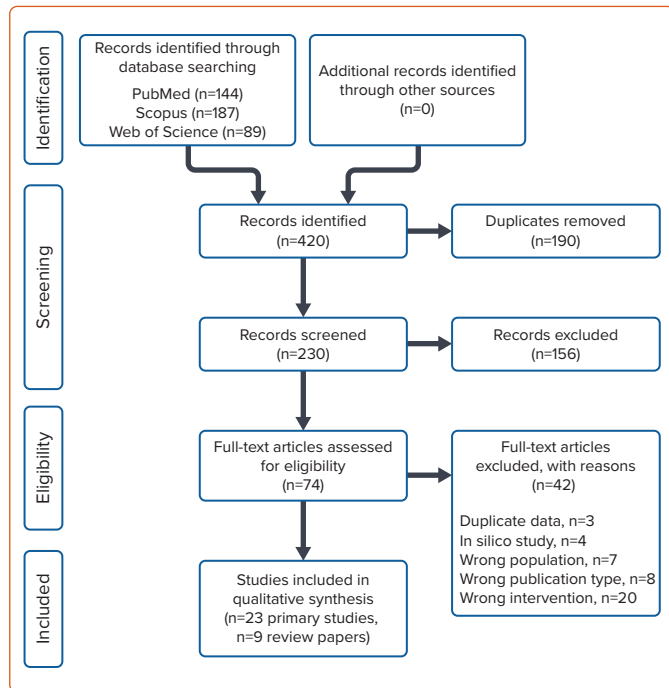
Given that the body surface potential mapping (BSPM) and ECGI methods are used mostly in the research field rather than in clinical settings, no standardised terminology concerning the specification of approaches exists. For this review, the methods related to the analysis and interpretation of body surface multi-lead ECG are referred to as BSPM. Techniques involved in the reconstruction of myocardial electrical potentials using body surface ECGs are termed ECGI.

### Methods

A systematic literature review was carried out to evaluate the available clinical evidence regarding non-invasive cardiac mapping methods for patient selection, lead placement, and optimisation of CRT programming. The preferred reporting items for systematic reviews and meta-analyses (PRISMA) statement was used as a basis for this review.<sup>6</sup>

In this review, we included randomised controlled trials and observational studies, such as cohort studies or case–control studies. Conference

Figure 1: PRISMA Flow Diagram



abstracts, letters and case reports were excluded. To cover all available evidence, we did not use any publication date restrictions.

The search was conducted using MEDLINE (through PubMed), Web of Science and Scopus databases. No limits were applied to language and foreign papers were translated. The reference lists of all included publications were checked to identify additional relevant studies. We also examined any relevant retraction statements and errata for the included studies.

The search terms included 'CRT', 'BSPM', 'ECGI', 'electrocardiographic mapping (ECM)', 'congestive HF', 'HFref', and various combinations of these terms. The full search strategies are given in the *Supplementary Material*.

The selected review publications were used to identify other publications not covered by our search. From the original studies included in the qualitative analysis, we extracted the following characteristics for each included study: participants (number of participants, target population); BSPM type (ECGI or simple BSPM); and BSPM parameters (definition and findings).

Duplicate articles were identified and excluded. Title and abstract screening for eligibility was performed by two reviewers independently. The full text of citations judged as potentially eligible was retrieved and screened in a blinded manner. The disagreement between the reviewers was then resolved by discussion or, if required, with the help of a third independent reviewer.

## Results

### Search Results

The literature search was performed on 21 January 2020. In total, 420 publications were identified in the main sources (PubMed, Scopus, and Web of Science). After the title and abstract screening, 156 records were excluded. The full text of 74 records was assessed for eligibility, and 23

original studies met the inclusion criteria. The procedure for selecting publications is shown in the PRISMA diagram (Figure 1).

Table 1 summarises the 23 selected original studies in the population, intervention, control and outcomes (PICO) format.<sup>3,5,7–27</sup> They include both BSPM (n=8) and ECGI methods (n=15). The median number of body surface leads used for ECGI was higher than for BSPM techniques (252 [IQR 192–252] versus 64 [IQR 53–87], respectively,  $p < 0.0001$ ). Non-invasive cardiac mapping approaches were applied in patients with CRT in several scenarios: the prediction of CRT response and patient selection; the selection of optimal LV pacing site; and the optimisation of CRT programming. Quantitative parameters of ventricular depolarisation are listed in Table 2. BSPM characteristics of depolarisation were mostly based on the detection of activation time, defined as the minimum of the first derivative of potential with respect to time during the QRS complex in unipolar body surface ECG leads. Parameters of ventricular activation obtained from reconstructed epicardial electrical potentials using ECGI techniques included local characteristics of ventricular depolarisation such as LV activation time, the interventricular difference in activation time, and intraventricular activation time distribution (Figure 2).

### Patient Selection for CRT

Current European Society of Cardiology guidelines approve CRT as an indication for patients with symptomatic HFref and intraventricular conduction abnormality, especially QRS duration  $>150$  ms and left bundle branch block (LBBB) morphology. In contrast, patients with QRS duration  $<120$ – $130$  ms are not indicated for CRT, due to a low success rate and possible worsening of HF.<sup>21,28</sup>

Assessment of electrical dyssynchrony is important for the accurate identification of appropriate CRT candidates. Although QRS duration is used as an indirect measure of dyssynchrony, some studies noted a weak correlation between QRS duration and mechanical dyssynchrony.<sup>29,30</sup> BSPM and ECGI approaches have been applied in clinical studies to develop reliable parameters of ventricular activation for assessment of the CRT effects (Table 2).

### BSPM-based Selection Criteria

BSPM-derived activation time (AT) is the duration between the QRS complex onset and the steepest negative slope of the QRS complex.<sup>3</sup> This can then be visualised as body surface isochronal maps of ATs. The isochronal maps of ATs have been obtained using BSPM with 53 ECG leads to assess the changes in electrical dyssynchrony in patients with CRT. Quantitative metrics of dyssynchrony such as the standard deviation of activation times (SDAT) and average left thorax activation time (LTAT) have been suggested. Patients with native SDAT  $\geq 35$  ms and QRS duration  $\geq 120$  ms had significant reverse LV remodelling (improvement in left ventricular ejection fraction [LVEF] and decrease in end-systolic volume), thus both parameters have been suggested as predictors of CRT response.<sup>3</sup> The longest activation time ( $AT_{max}$ ) detected in any of 123 unipolar chest leads, served as a reliable dyssynchrony marker to predict CRT outcome.<sup>14</sup> The right ventricular to left ventricular (RV–LV) activation gradient was identified through measures of QRS durations in 87-lead BSPM. It was suggested that an RV–LV activation gradient  $<20$  ms during biventricular pacing could identify patients with improved functional class after CRT.<sup>23</sup>

In our pilot study, an analysis of ventricular depolarisation was performed during different pacing configurations in selected patients using the QRS integral maps produced from a 96-lead mapping system (unpublished data). A 46-year-old patient with a history of post-myocarditis

Table 1: Summary of Included Original Studies

Objective	Population	n	Intervention, No. of Leads
<b>CRT optimisation</b>			
Bank et al. 2018 <sup>8</sup>	69 ± 11 years; 68% men; EF 26 ± 7%; QRSd 159 ± 23 ms; MI 50%; LBBB 62%	94	BSPM, 53
Berger et al. 2005 <sup>9</sup>	61 ± 8 years; 76% men; EF 21 ± 5%; QRSd 150 ± 24 ms; MI 44%; LBBB 100%	25	BSPM, 64
Lumens et al. 2013 <sup>15</sup>	66 ± 12 years; 71% men; EF 27 ± 3%; QRSd 164 ± 22 ms; MI 33%	24	ECGI, 252
Pastore et al. 2006 <sup>17</sup>	61 ± 9 years; 71% men; EF 28 ± 8%; QRSd 180 ± 19 ms; MI 11%; LBBB 100%	28	BSPM, 87
Pereira et al. 2018 <sup>18</sup>	68 ± 13 years; 79% men; MI 63%; LBBB 74%	19	ECGI, 252
Pereira et al. 2019 <sup>19</sup>	69 ± 12 years; 81% men; EF 27 ± 10%; QRSd 162 ± 21 ms; MI 62%; LBBB 71%	21	ECGI, 252
Samesima et al. 2013 <sup>24</sup>	61 ± 10 years; 60% men; EF 28 ± 9%; QRSd 182 ± 24 ms; MI 20%	55	BSPM, 87
Sieniewicz et al. 2019 <sup>26</sup>	61 ± 13 years; 80% men; EF 28 ± 9%; QRSd 168 ± 8 ms; MI 80%; LBBB 80%	5	ECGI, 252
<b>LV lead positioning</b>			
Arnold et al. 2018 <sup>7</sup>	67 ± 10 years; 53% men; EF 26 ± 7%; QRSd 158 ± 21 ms (BiV pacing); MI 38%; LBBB 100%	23	ECGI, 252
Ghosh et al. 2011 <sup>11</sup>	51 ± 18 years; 44% men; EF 22 ± 5%; QRSd 138 ± 27 ms; MI 0%;	25	ECGI, NA
Johnson et al. 2017 <sup>13</sup>	65 ± 14 years; 75% men; EF 27 ± 7%; QRSd 165 ± 26 ms; MI 40%; LBBB 58%	60	BSPM, 53
Nguyen et al. 2019 <sup>16</sup>	71 ± 8 years; 81% men; EF 24 ± 8%; QRSd 142 ± 21 ms; MI 69%; LBBB 38%	16	ECGI, 184
Rudy 2006 <sup>22</sup>	72 ± 11 years; 75% men	8	ECGI, 220 - 250
Varma 2014 <sup>27</sup>	54 ± 15 years; 33% men; EF 18 ± 3%; QRSd 146 ± 7 ms; MI 33%; LBBB 66%	3	ECGI, >200
<b>Patient selection</b>			
Dawoud et al. 2016 <sup>10</sup>	63 ± 10 years; 75% men; EF 20 ± 5%; QRSd 149 ± 9 ms; MI 37%; LBBB 100%	8	ECGI, 120
Gage et al. 2017 <sup>3</sup>	70 ± 11 years; 67% men; EF 27 ± 7%; QRSd 152 ± 26 ms; MI 48%; LBBB 55%	66	BSPM, 53
Jia et al. 2006 <sup>12</sup>	72 ± 11 years; 75% men; EF 19 ± 7%; QRSd 155 ± 22 ms; MI 75%; LBBB 75%;	8	ECGI, NA
Kittnar et al. 2018 <sup>44</sup>	62 ± 6 years; 57% men; EF 25 ± 8%; QRSd 170 ± 12 ms; LBBB 52%;	21	BSPM, NA
Ploux et al. 2013 <sup>20</sup>	65 ± 9 years; 85% men; EF 27 ± 4%; QRSd 152 ± 22 ms; MI 42%; LBBB 55%	33	ECGI, 252
Ploux et al. 2015 <sup>21</sup>	65 years (median); 80% men; EF 28%(median); QRSd 146 ms (median); MI 46%; LBBB 43%	61	ECGI, 252
Samesima et al. 2007 <sup>23</sup>	60 ± 11 years; 62% men; EF 31 ± 8%; QRSd 185 ± 35 ms; MI 18%; LBBB 100%	56	BSPM, 87
Shannon et al. 2008 <sup>25</sup>	64 ± 12 years; 71% men; MI 56%	34	ECGI, 80
Strik et al. 2018 <sup>5</sup>	67 ± 10 years; 78% men; EF 29 ± 5%; MI 48%; LBBB 51%	79	ECGI, 252

Data given as mean ± SD if not otherwise specified. BSPM = body surface potential mapping; ECGI = ECG imaging; EF = ejection fraction; LBBB = left bundle branch block; NA = not available; QRSd = QRS duration.

cardiomyopathy, LBBB (QRS 172 ms) and progressive LV dysfunction (LVEF 30%) underwent permanent CRT defibrillator (CRT-D) implantation in 2019, leading to reverse remodelling 6 months after CRT-D implantation (improvement of LVEF to 45%). The distribution of positive and negative time integrals correlated with the acute haemodynamic response to the different pacing configurations. Obtained time integral maps of the QRS complex reflected the improvement in LVEF during LV pacing compared with atrial pacing (Figure 3).

### ECGI-based Selection Criteria

In patients with LBBB and non-specific intraventricular conduction disturbance (NICD), an ECGI-derived index of electrical dyssynchrony, ventricular electric uncoupling (VEU), defined as the difference between the mean epicardial LV and RV activation times, served as a significant predictor of response to CRT. It was concluded that in consecutive CRT candidates with QRS duration ≥120 ms, VEU is a more reliable predictor of clinical CRT response than QRS duration or the presence of LBBB.<sup>20</sup> Supporting data were obtained in the study in which VEU was calculated at baseline and during biventricular pacing to assess the resynchronising effect in relation to the underlying electrical substrate. Responders had higher baseline VEU and more intensive reduction of VEU in response to biventricular pacing than did non-responders.<sup>21</sup>

Given that VEU represents the impairment of ventricular depolarisation only with regard to time, an activation delay vector (ADV) adds an additional parameter: a direction in space. This parameter represents a comprehensive electrical substrate, such that patients may have a similar direction of activation delay but a great difference in its magnitude. This parameter might be used to determine right-to-left activation delay and identify responders.<sup>5</sup>

Electrical synchrony of ventricles was assessed using isochronal activation maps obtained with the ECGI technique. The interventricular synchrony index, Esyn (the difference between activation times in the RV and LV), for estimation of electrical synchrony, however, did not always correlate with clinical improvement.<sup>12</sup> In that case, a non-invasive ECGI approach for reconstruction of epicardial ventricular activation was then applied, in combination with cardiac magnetic resonance used for mechanical imaging of dyssynchrony in the LV. Electromechanical dissociation has been suggested as a marker of reduced response to CRT.<sup>10</sup>

Spatiotemporal myocardial activation maps were constructed using the ECGI method in patients with wide QRS complex before CRT. The different patterns of myocardial activation described suggested an association between electrophysiological pattern and the effect of CRT.<sup>25</sup>

**Table 2: Parameters of Ventricular Activation Derived from Body Surface Potential Mapping or ECG Imaging**

Reference	Parameters
<b>BSPM</b>	
Bank et al. 2018 <sup>8</sup>	SDAT
Gage et al. 2017 <sup>3</sup>	SDAT, LTAT
Johnson et al. 2017 <sup>13</sup>	SDAT, LTAT
Kittnar et al. 2018 <sup>14</sup>	AT <sub>max</sub> , AT <sub>min</sub>
Pastore et al. 2006 <sup>17</sup>	mAS, mLv, mRV
Samesima et al. 2007 <sup>23</sup>	Global VAT, regional VAT, RV–LV VAT difference
Samesima et al. 2013 <sup>24</sup>	Global VAT, regional VAT, RV–LV VAT difference
<b>ECGI</b>	
Arnold et al. 2018 <sup>7</sup>	LVAT, LVAT-95, LVDI
Ghosh et al. 2011 <sup>11</sup>	ED
Jia et al. 2006 <sup>12</sup>	Esyn
Lumens et al. 2013 <sup>15</sup>	AT <sub>LV</sub> , AT <sub>TOT</sub>
Pereira et al. 2018 <sup>18</sup>	TVaT, VaT <sub>10-90</sub>
Pereira et al. 2019 <sup>19</sup>	TVaT, VaT <sub>10-90</sub>
Ploux et al. 2013 <sup>20</sup>	LVTAT, RVTAT, VEU
Ploux et al. 2015 <sup>21</sup>	LVTAT, TAT, VEU
Rudy 2006 <sup>22</sup>	Esyn
Sieniewicz et al. 2019 <sup>26</sup>	VVsync, VVTAT, LVTAT, LVdisp
Strik et al. 2018 <sup>5</sup>	ADV
Varma 2014 <sup>27</sup>	LVTAT

ADV = activation delay vector; AT<sub>LV</sub> = left ventricular activation time; AT<sub>max</sub> = maximum activation time; AT<sub>min</sub> = minimum activation time; AT<sub>TOT</sub> = total ventricular activation time; BSPM = body surface potential mapping; ECGI = ECG imaging; ED = electrical dyssynchrony; Esyn = electrical synchrony index; LTAT = average left thorax activation time; LVAT = left ventricular activation time; LVAT-95 = left ventricular activation time spanning 95% of activations; LVDI = left ventricular dyssynchrony index; LVdisp = global left ventricular dispersion of activation; LVTAT = left ventricular total activation time; mAS = anterior septal area mean activation time; mLv = left ventricle mean activation time; mRV = right ventricle mean activation time; RVTAT = right ventricular total activation time; SDAT = standard deviation of activation times; TAT = total activation time; TVaT = total ventricular activation time; VAT = ventricular activation time; VaT<sub>10-90</sub> = ventricular activation time<sub>10-90</sub> (delay between the 10th and 90th percentiles of ventricular activation time); VEU = ventricular electrical uncoupling; VVsync = global right/left ventricular electrical synchrony.

In summary, the most promising predictors of response to CRT appear to be SDAT and LTAT, parameters that can be derived from BSPM, without the need for 3D imaging. These parameters are easy to obtain and analyse.

### LV Lead Placement

The degree of cardiac resynchronisation response is influenced by many factors, of which the position of the LV lead on the heart is an important one. Many strategies have been used to optimise LV lead placement. Some of them use QLV interval, that is, the time between Q onset on the ECG and local depolarisation at the LV electrode, as measured during implantation, to determine the site of the latest activation. Other strategies involve echocardiography or MRI to evaluate the proximity of the lead to the site of maximal mechanical dyssynchrony.

### BSPM-based LV Lead Placement

More recently, BSPM has been suggested as another alternative for LV lead positioning.<sup>2,13</sup> The pacing site with the greatest decrease in SDAT and LTAT has been shown to have a strong correlation with the acute haemodynamic response measured invasively.<sup>13</sup>

### ECGI-based LV Lead Placement

In patients with a quadripolar LV lead, ECGI visualisation of endocardial and epicardial activation was applied to identify the optimal area for pacing, that is, the site with the shortest total activation duration of both ventricles.<sup>27,31</sup> ECGI isochronal maps of epicardial ventricular depolarisation also enabled the guidance of LV lead placement for improved clinical outcome.<sup>22</sup> Another study integrated ECGI with CT angiography and cardiac magnetic resonance to develop the ‘CRT roadmap’, which provides data on scar localisation, epicardial activation sequence, and coronary venous anatomy. This CRT roadmap was suggested to be a reliable tool to guide LV lead placement.<sup>16</sup>

In some cases, LV lead placement is suboptimal due to unfavourable anatomy of the coronary venous system, and the response to CRT may be inferior.<sup>32</sup> Recently, His bundle pacing (HBP) has emerged as an alternative to CRT. With the help of ECGI, it was established that HBP reduced LV activation time and LV dyssynchrony index (LVDI) more than twofold compared with biventricular pacing.<sup>7,11</sup> The His-SYNC (His Bundle Pacing versus Coronary Sinus Pacing for Cardiac Resynchronisation Therapy) pilot trial was an investigator-initiated, prospective, randomised controlled study that demonstrated that there were no significant improvements in ECG or echocardiographic parameters compared with biventricular pacing-CRT.<sup>33</sup>

### Optimisation of CRT Programming

LV pacing and biventricular pacing have a similar, positive effect on the haemodynamic function of patients with HF, while RV pacing alone is highly ineffective.<sup>12,17,22,34</sup>

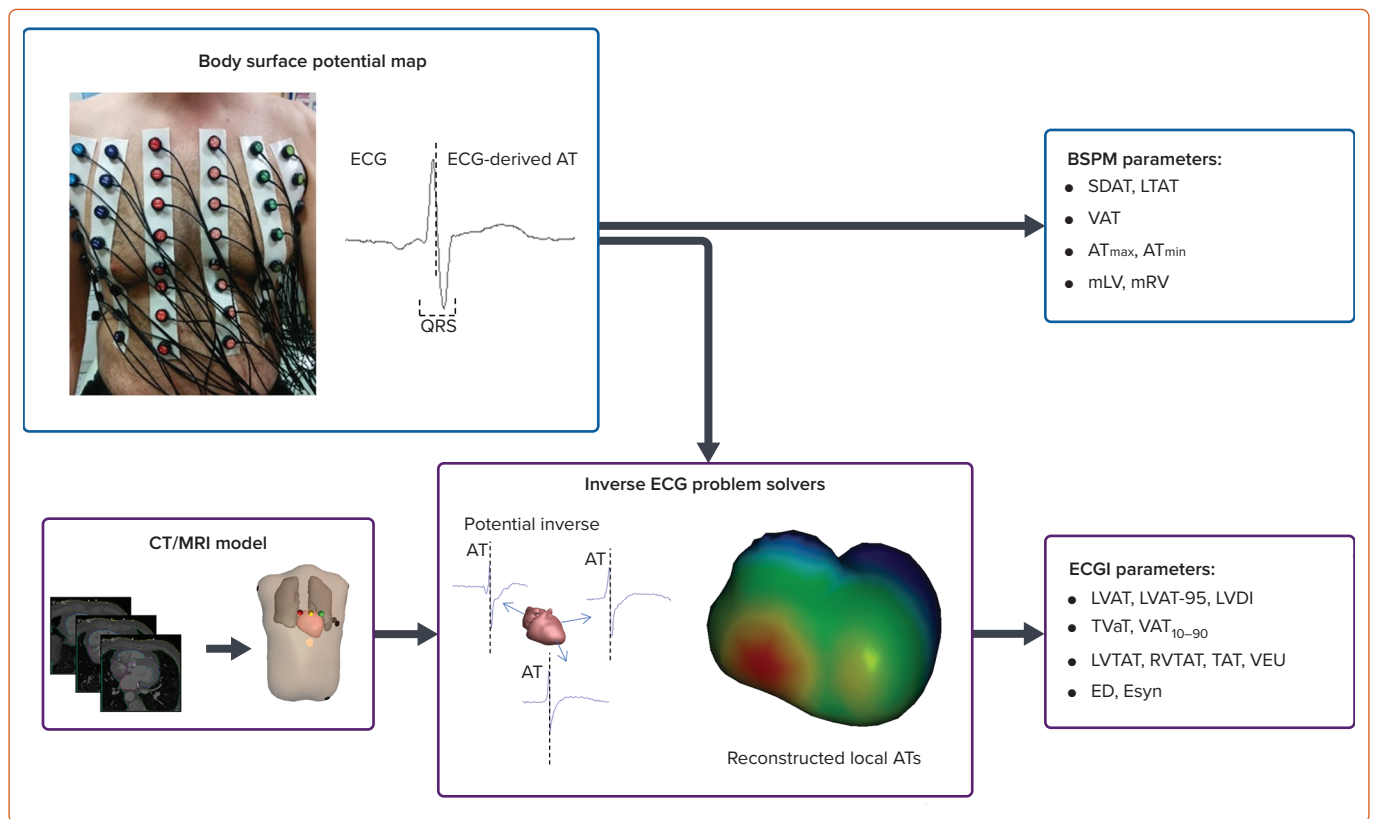
### BSPM-based CRT Optimisation

BSPM parameters such as SDAT can be useful for both LV pacing and biventricular pacing programming.<sup>8</sup> CRT programmed at baseline settings can reduce dyssynchrony by up to 20%. This improvement is greater in the LBBB group of patients with wide QRS, and is lacking in the non-LBBB group. However, individualised and optimised settings based on BSPM parameters, such as SDAT, can further improve ventricular activation time by 46%, compared with standard pacing settings.<sup>3</sup> SDAT reduction  $\geq 10\%$  was a significant predictor of improved ejection fraction and LV end-systolic volume response. With CRT optimisation, it is possible to achieve twofold improvement in electrical synchrony, regardless of patient baseline characteristics.<sup>8</sup> Another BSPM approach based on measurement of QRS duration in 87 body surface unipolar leads showed that regional activation time in the RV increased in biventricular pacing, but it was compensated for by an even greater decrease in activation time in the LV, therefore the effect of CRT could be optimised by decreasing the inter-regional RV–LV gradients.<sup>23,24</sup> In addition, BSPM parameters of ventricular repolarisation dispersion such as T<sub>peak</sub>–T<sub>end</sub> interval, T<sub>peak</sub>–T<sub>end</sub> integral, and T wave amplitude were reduced compared with sinus rhythm under biventricular pacing, whereas RV or LV pacing resulted in increased dispersion of repolarisation.<sup>9</sup>

### ECGI-based CRT Optimisation

Using ECGI techniques to reconstruct epicardial isochronal maps, it has been shown that, despite the positive haemodynamic response during LV pacing, only biventricular pacing has resulted in reduced electrical dyssynchrony, represented by decreased total RV and LV activation time.<sup>15</sup> The individual configuration of LV quadripolar leads guided by the parameters total ventricular activation time (TVaT) and the time for the bulk of ventricular activation (VaT<sub>10-90</sub>), which were obtained from ECGI,

Figure 2: Schematic Presentation of BSPM and ECGI Approaches to Determine Electrical Synchrony in Heart Ventricles



Body surface electrodes are applied to the patient's torso for simultaneous recording of 52–252 unipolar ECG leads using a multichannel ECG recording system. For the body surface potential mapping (BSPM) approach, each ECG signal is processed to determine specific signal features, for example duration and amplitude of the Q, R, and S waves, and ECG-derived activation time (AT,  $dV/dt_{min}$  during the QRS complex). Based on these quantitative parameters the ventricular electrical dyssynchrony is estimated. For ECG imaging (ECGI) methods, thoracic CT or MRI is used to provide the patient-specific anatomical model of cardiac geometry and torso-electrode positions. Body surface ECGs and CT or MRI model data are combined in the inverse procedure to obtain non-invasive ECGI epicardial electrograms (blue lines) and isochronal activation sequences (colour-coded reconstructed myocardial ATs on the heart surface).

AT<sub>max</sub> = maximum activation time; AT<sub>min</sub> = minimum activation time; ED = electrical dyssynchrony; E<sub>syn</sub> = electrical synchrony index; LTAT = average left thorax activation time; LVAT = left ventricular activation time; LVAT-95 = left ventricular activation time spanning 95% of activations; LVDI = left ventricular dyssynchrony index; LVTAT = left ventricular total activation time; mLV = left ventricle mean activation time; mRV = right ventricle mean activation time; RVTAT = right ventricular total activation time; SDAT = SD of activation times; TAT = total activation time; TVaT = total ventricular activation time; VAT = ventricular activation time; VaT<sub>10-90</sub> = ventricular activation time<sub>10-90</sub> (delay between the 10th and 90th percentiles of ventricular activation time); VEU = ventricular electrical uncoupling.

significantly increased the resynchronisation effect in both ischaemic and non-ischaemic patients.<sup>18</sup> The aforementioned parameters, TVaT and VaT<sub>10-90</sub>, were also used to identify the optimal atrioventricular delay (AVD) and interventricular pacing interval (VVD). The minimum TVaT and VaT<sub>10-90</sub> values were associated with the most improved ventricular haemodynamics, suggesting that ECG mapping approaches are effective for programming optimisation.<sup>19</sup> The potential of ECGI activation maps for detection of the best configuration of multi-polar pacing was demonstrated in a pilot study with five patients.<sup>26</sup>

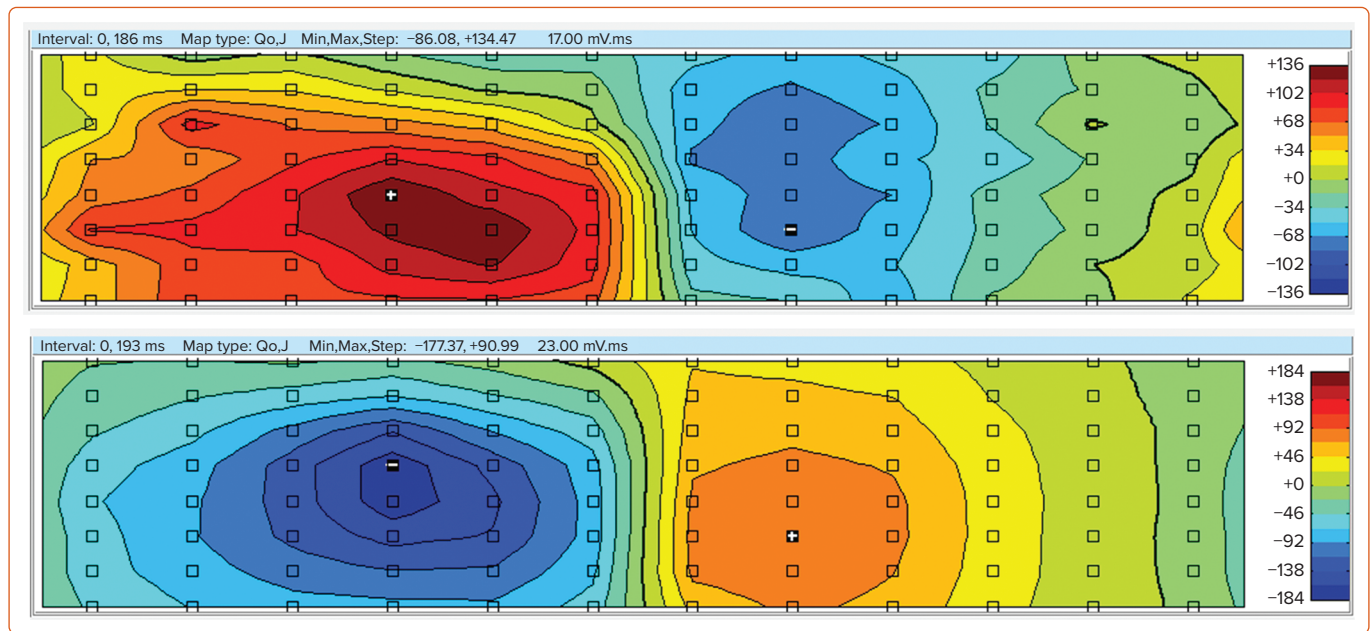
## Discussion

One of the therapeutic options for advanced management of HF<sub>rEF</sub> patients during the last 30 years has been CRT. To increase the efficiency of CRT, different approaches have been applied, such as clinical and experimental approaches, and computer simulation. The experimental porcine model of LBBB to induce electrical and mechanical dyssynchrony was suggested for the study of the mechanisms of CRT effect in a treatment of HF.<sup>35</sup> Preclinical studies, including both animal experimental models and patient-specific computational models of the heart, demonstrate a high potential for prediction and optimisation of CRT treatment. Nevertheless, clinical studies are required to validate the efficacy of these models in the target HF population, as well as the applicability of these models to the ECGI methods discussed in this work.<sup>36</sup>

BSPM could be useful for the selection of HF<sub>rEF</sub> patients with a borderline QRS width on standard ECG. Most of the evidence suggests that SDAT  $\geq 35$  ms from BSPM with 53 leads can predict reverse LV remodelling after CRT, as can the greater change of SDAT ( $\Delta$ SDAT) from baseline to post-implant values. ECGI can further improve patient selection with the use of parameters such as ADV or VEU. BSPM has been advocated as an alternative guide for the positioning of the LV lead during the implant procedure. It is based on the presumption that choosing the pacing site with the greatest reduction in SDAT will correspond to an improvement in haemodynamics as evaluated using invasive measurement of acute haemodynamic response. However, there is no comparison between these BSPM-derived parameters and the simple strategy, such as the selection of the pacing site based on the identification of the late local activation in sinus rhythm. In our opinion, BSPM has a large potential for individualising the optimisation of CRT device programming. This conclusion is based on studies showing that the optimised SDAT parameter is predictive of reverse remodelling, regardless of the baseline characteristics of the CRT candidates.

As an alternative to BSPM, a novel approach based on ultra-high-frequency ECG was recently suggested to improve patient selection for CRT treatment. Jurak et al. demonstrated that an ultra-high-frequency 14-lead ECG technique could improve the application of CRT based on new

Figure 3: QRS Integral Maps of a Patient with Heart failure Under Atrial Pacing (Top) and Left Ventricular Pacing (Bottom)



Distribution of 96 torso electrodes in the QRS time integral maps. The left and right sides of each map correspond to the anterior and posterior torso aspects, respectively. Maximum and minimum are marked by plus and minus signs, respectively.

ECG indices of ventricular depolarisation.<sup>37</sup> This technique may prove to be a valuable addition to the discussed BSPM and ECGI methods.

Artificial intelligence techniques have recently been proposed as a promising tool in cardiac electrophysiology to increase the diagnostic accuracy and treatment capabilities of medical technologies such as surface ECG, intracardiac mapping and cardiac implantable electronic devices.<sup>38,39</sup> A machine learning model with nine variables demonstrated improved CRT response prediction compared with guidelines.<sup>40</sup> Kalscheur et al. developed a random forest model that predicted all-cause mortality and HF hospitalisation in patients receiving CRT implantation, based on pre-implant characteristics.<sup>41</sup> Hu et al. successfully applied machine learning techniques with natural language processing to identify a subgroup of patients who were unlikely to benefit from CRT.<sup>42</sup> Machine learning models that relied on pre-implantation clinical, echocardiographic, and ECG characteristics produced understandably better predictions of CRT benefit than those that relied on ECG parameters.<sup>41,42</sup> This integration approach based on analysis of many clinical parameters may provide a new opportunity for personalised management of patients with HF. The combination of ECGI-derived parameters and machine learning models may provide a pathophysiological interpretation of related clinical features and CRT response.

An advantage of ECGI methods relates to the ability to obtain important information on CRT effect through an electrical solution to a mechanical problem. A solid understanding of the electromechanical structure of the heart is required. Future ECGI developments should therefore aim to increase the modelling capabilities used in ECG technology to reduce the

number of required ECG leads, preferably to the standard 12-lead ECG configuration. Recent developments in the anatomical localisation of premature ventricular contractions from a 12-lead ECG using ECGI technology show that the potential of the ECGI technology has not been fully explored.<sup>43</sup>

### Conclusion

BSPM and ECGI can be used in CRT in several ways. There is a potential for improvement of patient selection for CRT, optimisation of CRT programming and LV lead placement. The most promising parameter (and also the easiest to obtain) is SDAT derived from BSPM. Further prospective or randomised trials are necessary to identify the utility of BSPM for routine clinical practice. □

### Clinical Perspective

- For clinical use, the standard deviation of activation times appears to be the most promising parameter for individualised optimisation of CRT device programming without the need for imaging studies.
- Further prospective or randomised trials are necessary to verify the utility of body surface potential mapping for routine clinical practice.
- ECG imaging approaches can provide detailed information on the depolarisation process in ventricles with heart failure, which is crucial for understanding the relationship between electromechanical status and CRT effect.

1. Thomas G, Kim J, Lerman BB. Improving cardiac resynchronization therapy. *Arrhythm Electrophysiol Rev* 2019;8:220–7. <https://doi.org/10.15420/aer.2018.62.3>; PMID: 31463060.
2. Pujol-Lopez M, San Antonio R, Mont L, et al. Electrocardiographic optimization techniques in resynchronization therapy. *Europace* 2019;21:1286–96. <https://doi.org/10.1093/europace/euz126>; PMID: 31038177.
3. Gage RM, Curtin AE, Burns KV, et al. Changes in electrical dyssynchrony by body surface mapping predict left ventricular remodeling in cardiac resynchronization therapy patients. *Heart Rhythm* 2017;14:392–9. <https://doi.org/10.1016/j.hrthm.2016.11.019>; PMID: 27867072.
4. Bear LR, Huntjens PR, Walton RD, et al. Cardiac electrical dyssynchrony is accurately detected by noninvasive electrocardiographic imaging. *Heart Rhythm* 2018;15:1058–69. <https://doi.org/10.1016/j.hrthm.2018.02.024>; PMID: 29477975.
5. Strik M, Ploux S, Huntjens PR, et al. Response to cardiac resynchronization therapy is determined by intrinsic electrical substrate rather than by its modification. *Int J Cardiol* 2018;270:143–8. <https://doi.org/10.1016/j.ijcard.2018.06.005>; PMID: 29895424.
6. Moher D, Liberati A, Tetzlaff J, Altman DG. Preferred

- reporting items for systematic reviews and meta-analyses: the PRISMA statement. *PLoS Med* 2009;6:e1000097. <https://doi.org/10.1371/journal.pmed.1000097>; PMID: 19621072.
7. Arnold AD, Shun-Shin MJ, Keene D, et al. His resynchronization versus biventricular pacing in patients with heart failure and left bundle branch block. *J Am Coll Cardiol* 2018;72:3112–22. <https://doi.org/10.1016/j.jacc.2018.09.073>; PMID: 30554540.
  8. Bank AJ, Gage RM, Curtin AE, et al. Body surface activation mapping of electrical dyssynchrony in cardiac resynchronization therapy patients: potential for optimization. *J Electrocardiol* 2018;51:534–41. <https://doi.org/10.1016/j.jelectrocard.2017.12.004>; PMID: 29273234.
  9. Berger T, Hanser F, Hintringer F, et al. Effects of cardiac resynchronization therapy on ventricular repolarization in patients with congestive heart failure. *J Cardiovasc Electrophysiol* 2005;16:611–17. <https://doi.org/10.1046/j.1540-8167.2005.40496.x>; PMID: 15946359.
  10. Dawoud F, Spragg DD, Berger RD, et al. Non-invasive electromechanical activation imaging as a tool to study left ventricular dyssynchronous patients: implication for CRT therapy. *J Electrocardiol* 2016;49:375–82. <https://doi.org/10.1016/j.jelectrocard.2016.02.011>; PMID: 26968312.
  11. Ghosh S, Silva JNA, Canham RM, et al. Electrophysiologic substrate and intraventricular left ventricular dyssynchrony in nonischemic heart failure patients undergoing cardiac resynchronization therapy. *Heart Rhythm* 2011;8:692–9. <https://doi.org/10.1016/j.hrthm.2011.01.017>; PMID: 21232630.
  12. Jia P, Ramanathan C, Ghanem RN, et al. Electrocardiographic imaging of cardiac resynchronization therapy in heart failure: observation of variable electrophysiologic responses. *Heart Rhythm* 2006;3:296–310. <https://doi.org/10.1016/j.hrthm.2005.11.025>; PMID: 16500302.
  13. Johnson WB, Vatterott PJ, Peterson MA, et al. Body surface mapping using an ECG belt to characterize electrical heterogeneity for different left ventricular pacing sites during cardiac resynchronization: relationship with acute hemodynamic improvement. *Heart Rhythm* 2017;14:385–91. <https://doi.org/10.1016/j.hrthm.2016.11.017>; PMID: 27871987.
  14. Kittnar O, Riedlbauchova L, Adla T, et al. Outcome of resynchronization therapy on superficial and endocardial electrophysiological findings. *Physiol Res* 2018;67:601–10. <https://doi.org/10.33549/physiolres.934056>; PMID: 30607967.
  15. Lumens J, Ploux S, Strik M, et al. Comparative electromechanical and hemodynamic effects of left ventricular and biventricular pacing in dyssynchronous heart failure: electrical resynchronization versus left-right ventricular interaction. *J Am Coll Cardiol* 2013;62:2395–403. <https://doi.org/10.1016/j.jacc.2013.08.715>; PMID: 24013057.
  16. Nguyen UC, Cluitmans MJM, Strik M, et al. Integration of cardiac magnetic resonance imaging, electrocardiographic imaging, and coronary venous computed tomography angiography for guidance of left ventricular lead positioning. *Europace* 2019;21:626–35. <https://doi.org/10.1093/europace/euy292>; PMID: 30590434.
  17. Pastore CA, Tobias N, Samesima N, et al. Body surface potential mapping investigating the ventricular activation patterns in the cardiac resynchronization of patients with left bundle-branch block and heart failure. *J Electrocardiol* 2006;39:93–102. <https://doi.org/10.1016/j.jelectrocard.2005.07.004>; PMID: 16387060.
  18. Pereira H, Jackson TA, Sieniewicz B, et al. Non-invasive electrophysiological assessment of the optimal configuration of quadripolar lead vectors on ventricular activation times. *J Electrocardiol* 2018;51:714–19. <https://doi.org/10.1016/j.jelectrocard.2018.05.006>; PMID: 29997019.
  19. Pereira H, Jackson TA, Claridge S, et al. Comparison of echocardiographic and electrocardiographic mapping for cardiac resynchronization therapy optimisation. *Cardiol Res Pract* 2019;2019:4351693. <https://doi.org/10.1155/2019/4351693>; PMID: 30918721.
  20. Ploux S, Lumens J, Whinnett Z, et al. Noninvasive electrocardiographic mapping to improve patient selection for cardiac resynchronization therapy: beyond QRS duration and left bundle branch block morphology. *J Am Coll Cardiol* 2013;61:2435–43. <https://doi.org/10.1016/j.jacc.2013.01.093>; PMID: 23602768.
  21. Ploux S, Eschaliier R, Whinnett ZI, et al. Electrical dyssynchrony induced by biventricular pacing: implications for patient selection and therapy improvement. *Heart Rhythm* 2015;12:782–91. <https://doi.org/10.1016/j.hrthm.2014.12.031>; PMID: 2554681.
  22. Rudy Y. Noninvasive electrocardiographic imaging of cardiac resynchronization therapy in patients with heart failure. *J Electrocardiol* 2006;39:28–30. <https://doi.org/10.1016/j.jelectrocard.2006.03.012>; PMID: 16950331.
  23. Samesima N, Douglas R, Tobias N, et al. Twenty-millisecond interventricular difference as assessed by body surface potential mapping identifies patients with clinical improvement after implantation of cardiac resynchronization device. *Anadolu Kardiyol Derg* 2007;7(Suppl 1):213–5. PMID: 17584728.
  24. Samesima N, Pastore CA, Douglas RA, et al. Improved relationship between left and right ventricular electrical activation after cardiac resynchronization therapy in heart failure patients can be quantified by body surface potential mapping. *Clinics* 2013;68:986–91. [https://doi.org/10.6061/clinics/2013\(07\)16](https://doi.org/10.6061/clinics/2013(07)16); PMID: 23917664.
  25. Shannon J, Navarro CO, McEntee T, et al. An early phase of slow myocardial activation may be necessary in order to benefit from cardiac resynchronization therapy. *J Electrocardiol* 2008;41:531–5. <https://doi.org/10.1016/j.jelectrocard.2008.07.028>; PMID: 18817924.
  26. Sieniewicz BJ, Jackson T, Claridge S, et al. Optimization of CRT programming using non-invasive electrocardiographic imaging to assess the acute electrical effects of multipoint pacing. *J Arrhythm* 2019;35:267–75. <https://doi.org/10.1002/joa3.12153>; PMID: 31007792.
  27. Varma N. Variegated left ventricular electrical activation in response to a novel quadripolar electrode: visualization by non-invasive electrocardiographic imaging. *J Electrocardiol* 2014;47:66–74. <https://doi.org/10.1016/j.jelectrocard.2013.09.001>; PMID: 24099886.
  28. Sorgente A, Cappato R. A critical reappraisal of the current clinical indications to cardiac resynchronization therapy. *Arrhythm Electrophysiol Rev* 2013;2:91–4. <https://doi.org/10.15420/aer.2013.2.2.91>; PMID: 26835046.
  29. Auger D, Bleeker GB, Bertini M, et al. Effect of cardiac resynchronization therapy in patients without left intraventricular dyssynchrony. *Eur Heart J* 2012;33:913–20. <https://doi.org/10.1093/eurheartj/ehr468>; PMID: 22279110.
  30. Bleeker GB, Schalij MJ, Molhoek SG, et al. Relationship between QRS duration and left ventricular dyssynchrony in patients with end-stage heart failure. *J Cardiovasc Electrophysiol* 2004;15:544–9. <https://doi.org/10.1046/j.1540-8167.2004.03604.x>; PMID: 15149423.
  31. Seger M, Hanser F, Dichtl W, et al. Non-invasive imaging of cardiac electrophysiology in a cardiac resynchronization therapy defibrillator patient with a quadripolar left ventricular lead. *Europace* 2014;16:743–9. <https://doi.org/10.1093/europace/euu045>; PMID: 24798964.
  32. Lambiase PD, Rinaldi A, Hauck J, et al. Non-contact left ventricular endocardial mapping in cardiac resynchronization therapy. *Heart* 2004;90:44–51. <http://dx.doi.org/10.1136/heart.90.1.44>; PMID: 14676240.
  33. Upadhyay GA, Vijayaraman P, Nayak HM, et al. His corrective pacing or biventricular pacing for cardiac resynchronization in heart failure. *J Am Coll Cardiol* 2019;74:157–9. <https://doi.org/10.1016/j.jacc.2019.04.026>; PMID: 31078637.
  34. Vatasescu R, Berruazo A, Mont L, et al. Midterm 'super-response' to cardiac resynchronization therapy by biventricular pacing with fusion: insights from electro-anatomical mapping. *Europace* 2009;11:1675–82. <https://doi.org/10.1093/europace/eup333>; PMID: 19880850.
  35. Rigol M, Solanes N, Fernandez-Armenta J, et al. Development of a swine model of left bundle branch block for experimental studies of cardiac resynchronization therapy. *J Cardiovasc Trans Res* 2013;6:616–22. <https://doi.org/10.1007/s12265-013-9464-1>; PMID: 23636845.
  36. Lee AWC, Costa CM, Strocchi M, et al. Computational modeling for cardiac resynchronization therapy. *J Cardiovasc Trans Res* 2018;11:92–108. <https://doi.org/10.1007/s12265-017-9779-4>; PMID: 29327314.
  37. Jurak P, Curila K, Leinveber P, et al. Novel ultra-high-frequency electrocardiogram tool for the description of the ventricular depolarization pattern before and during cardiac resynchronization. *J Cardiovasc Electrophysiol* 2020;31:300–7. <https://doi.org/10.1111/jce.14299>; PMID: 31788894.
  38. Muthalaly RG, Evans RM. Applications of machine learning in cardiac electrophysiology. *Arrhythm Electrophysiol Rev* 2020;9:71–7. <https://doi.org/10.15420/aer.2019.19>; PMID: 32983527.
  39. van de Leur RR, Boonstra MJ, Bagheri A, et al. Big data and artificial intelligence: opportunities and threats in electrophysiology. *Arrhythm Electrophysiol Rev* 2020;9:146–54. <https://doi.org/10.15420/aer.2020.26>; PMID: 33240510.
  40. Feeny AK, Rickard J, Patel D, et al. Machine learning prediction of response to cardiac resynchronization therapy: improvement versus current guidelines. *Circ Arrhythm Electrophysiol* 2019;12:e007316. <https://doi.org/10.1161/CIRCEP.119.007316>; PMID: 31216884.
  41. Kalscheur MM, Kipp RT, Tattersall MC, et al. Machine learning algorithm predicts cardiac resynchronization therapy outcomes. *Circ Arrhythm Electrophysiol* 2018;11:e005499. <https://doi.org/10.1161/circep.117.005499>; PMID: 29326129.
  42. Hu S-Y, Santus E, Forsyth AW, et al. Can machine learning improve patient selection for cardiac resynchronization therapy? *PLoS One* 2019;14:e0222397. <https://doi.org/10.1371/journal.pone.0222397>; PMID: 31581234.
  43. Misra S, van Dam PM, Chrispin J, et al. Initial validation of a novel ECGI system for localization of premature ventricular contractions and ventricular tachycardia in structurally normal and abnormal hearts. *J Electrocardiol* 2018;51:801–8. <https://doi.org/10.1016/j.jelectrocard.2018.05.018>; PMID: 30177316.